Tellus (1992), *44B*, 390–408

Lower stratosphere waves during 1986–1989 Southern Springs

By JULIA NOGUÉS-PAEGLE, *Department of Meteorology, University of Utah, 819 Wm. C. Browning Building, Salt Lake City, Utah 84112, USA*, KINGTSE C. MO, *CAC/NMC/NOAA, Washington, D.C., 20233, USA* and KEVIN P. CALLAHAN, *Department of Meteorology, University of Utah, 819 Wm. C. Browning Building, Salt Lake City, Utah 84112, USA*

(Manuscript received 17 September 1991; in final form 18 March 1992)

ABSTRACT

This paper describes the horizontal structure of ozone and 50 mb height waves for the 1986–1989 springs of the Southern Hemisphere using global NMC height analyses and Nimbus 7 TOMS Grid-T Version 6 data. Empirical Orthogonal Functions (EOFs) are obtained for the ozone and height data independently to identify the meridional structure of observed long waves as well as their propagation characteristics. It is found that the leading EOFs for both the ozone and 50 mb height waves exhibit wavenumber 1 and 2 patterns. The wave 1 pattern is usually centered at 60–65° S and it either propagates eastward with a period of 30 days or longer (1986, 1987, 1989) or it is quasi-stationary (1988). This wave is weak during 1987, a year with low ozone values which persisted into summer. The wave 2 pattern travels eastward with a period of 10–12 days. It is best defined while the polar vortex is strong and its amplitude in the ozone field is observed to decay sharply after onset of the summer regime. The correlation coefficients between ozone and 50 mb height principal components are high. These indicate high/low ozone values associated with high/low values of 50 mb heights. This distribution is consistent with the advection of ozone by planetary waves south of the ozone maximum, as shown by a simple linear wave model. This model consists of an equivalent barotropic wave between 5 and 150 mb. The observed total ozone amplitudes for waves 1 and 2 for most years are consistent with the total ozone predictions by the wave model. In contrast, during 1989, a year with a well defined vertically propagating wave 1, the linear model overpredicts the observed ozone wave amplitude by a factor of 2.

1. Introduction

Recent observations of total column ozone during the 1991 Southern Hemisphere spring have continued to register depleted ozone levels over Antarctica. Preliminary analysis of Total Ozone Mapping Spectrometer (TOMS) on NASA Nimbus-7 satellite (e.g., Beasley, 1991) indicate that values as low as 110 Dobson units (DU) were observed last October. This constitutes the lowest value ever observed on an individual day. The chemically produced ozone hole is distorted by atmospheric waves which bring ozone depleted air of polar latitudes into mid-latitudes during winter. During spring, dramatic changes take place in ozone concentration and it is not obvious how much the planetary waves determine the day-to-day variations of ozone concentration. It is the purpose of this paper to quantify the relationship between these waves and the total column ozone content (as measured by the TOMS) for the years 1986 through 1989. This period includes the anomalous circulations of the 1987 and 1988 austral springs, when the circumpolar vortex exhibited very late and early demises, respectively.

Ozone concentration, defined as the ratio between the number of ozone to air molecules, increases rapidly with height maximizing at about 5 mb. The TOMS measures the vertically integrated ozone (number of ozone molecules per unit area). Since this total column value has large contributions from the ozone density in a vertical layer centered at about 22 km (height of mean maximum ozone density), it is expected that the horizontal distribution of total ozone would be largely due to air motions in the lower stratosphere. At these elevations, ozone behaves essentially as a passive tracer and therefore motions from the north over the southern polar region tend to advect air with higher ozone content from mid-latitudes. Conversely, flow from the ozone depleted polar cap will cause air with low ozone content to move into mid-latitudes. This meridional advection may be modified by vertical motions. Since ozone concentration increases with altitude rising/sinking motions in the lower stratosphere will cause a decrease/increase of ozone density. Whether the horizontal and vertical advections reinforce or cancel each other depends on the characteristics of atmospheric motions. For example, in the medium-scale waves (wave 5) discussed by Schoeberl and Krueger (1983), the horizontal advection is reinforced by vertical advection. These waves reach maximum amplitude at about 45° S, exhibit little vertical tilt and are trapped within the troposphere. In contrast, the present study focuses on planetary waves which maximize at about 60° S and which are known to propagate from the troposphere into the stratosphere during winter (e.g., Andrews et al., 1987). Such waves tilt towards the West with height and thus tend to weaken the vertically integrated ozone signal through compensating meridional advections at different altitudes. Total ozone may be used as an indicator of the vertically averaged wave pattern, indicating an essential barotropic wave structure when the total ozone and heights (at a given isobaric level) are in phase. On the other hand, ozone and height structures with coherent time variations but out of phase horizontal patterns indicate atmospheric waves which tilt in the vertical. This study documents the phase and amplitude characteristics of total ozone and 50 mb height waves for the 1986 through 1989 southern springs.

The seasonal evolution of the zonal mean maximum ozone concentration differs markedly in both hemispheres. In April, during Northern Hemisphere spring, the maximum ozone concentration is found over the polar cap, while in October during southern spring the maximum is found at mid-latitudes, whith lower values remaining at polar latitudes until very late in spring (Bowman and Krueger, 1985). These low polar values are associated with the cold strong circumpolar vortex observed at high southern latitudes until late spring and are partly due to the observed ozone depletion over Antarctica. The spring season is also characterized by a maximum in transient wave energy (e.g., Randel, 1987a) and therefore events of low ozone air moving into lower latitudes are potentially more likely to occur during this time.

Quantification of the relationship between ozone and height waves is also of practical significance. Currently, there are no operational models that predict the day-to-day changes of ozone, though integrations of general circulation models that include ozone as a passive tracer have been successful in simulating the climatological ozone distribution (Mahlman et al., 1980). Ozone prediction in shorter time scales requires development of complex numerical models which include the various feedbacks between dynamical, photochemical and radiative processes. Additionally, accurate coupling of tropospheric and stratospheric circulations is needed, particularly during the transition from spring to summer which requires the accurate simulation of upward wave propagation. Also, high horizontal resolution is important to correctly simulate sudden warmings, as shown by Mechoso et al. (1985) for the 1979 Northern Hemisphere warming. The increased computer power and advances in operational numerical models raises hopes for the accurate prediction of stratospheric motions. The present study constitutes a first step to quantify the relationship between total ozone and lower stratosphere height anomalies in the Southern Hemisphere. High correlation coefficients between these fields would allow prediction of potential large scale incursions of ozone depleted air from polar into mid-latitudes based on successful predictions of the lower stratosphere flow by numerical weather prediction models.

This paper documents prevailing patterns of ozone and 50 mb wave heights in the Southern Hemisphere and relates these to those observed in the upper troposphere. Global NMC height analysis at 8 levels (400, 300, 250, 200, 150, 100, 70 and 50 mb), tropopause heights from September 15 through December 15 and Nimbus 7 TOMS Grid-T Version 6 data for September 1 through December 31 for 1986, 87, 88 and 89 are used to quantify the relationships between these fields. The calibration method for the TOMS data is discussed in McPeters et al. (1990).

The paper is organized as follows. Section 2 describes the seasonal transition for the 1986 through 1989 austral springs and the general characteristics of total ozone and tropopause pressure waves as shown in longitude-time diagrams at 60° S. The analysis reveals the existence of waves 1 and 2 both in ozone and tropopause pressure. Low/high tropopause pressure is associated with low/high ozone levels. Correlation between tropopause pressure and heights, and between 50 mb heights and heights of seven other isobaric surfaces are computed to describe the vertical structure of waves. The horizontal structure of ozone and height waves is described based on empirical orthogonal functions (EOF) in section 3. The principal components (PC) between ozone and 50 mb heights are shown to be highly correlated until the beginning of summer. This correlation and observed phase differences in the horizontal patterns of ozone and heights are interpreted using a linearized form of the conservation equation for ozone mixing ratio presented in the Appendix. The high correlation coefficients between ozone and height PCs indicate the feasibility of extending predictions of total ozone based on height forecasts.

2. Interannual variability of planetary wave activity at 60°S

The fact that total ozone amount correlates negatively with tropopause height (positively with tropopause pressure) has been known for a long time (e.g., Meetham, 1937). Also, since upper tropospheric troughs are characterized by warm temperatures and low tropopause, tropopause height (pressure) is positively (negatively) correlated with heights of isobaric surfaces in the upper levels of the troposphere. Above the tropopause this relationship changes sign with warm air over upper level tropospheric troughs hydrostatically inducing ridges in the stratosphere. These relationships are quantified here for the 1986 through 1989 southern springs.

First, pressure-time diagrams of the zonally averaged zonal wind at 60° S are shown in Fig. 1 to describe the interannual variability of the polar vortex during the period of interest. The strong polar vortex of 1987, with its late demise near the end of November 1987, and the early warming of 1988 around mid-October, are apparent in these figures. The planetary wave activity for these four seasons was also quite different. This is quantified by computing the zonally asymmetric component (deviation from zonal average) of ozone and tropopause pressure anomalies at 60° S. This is

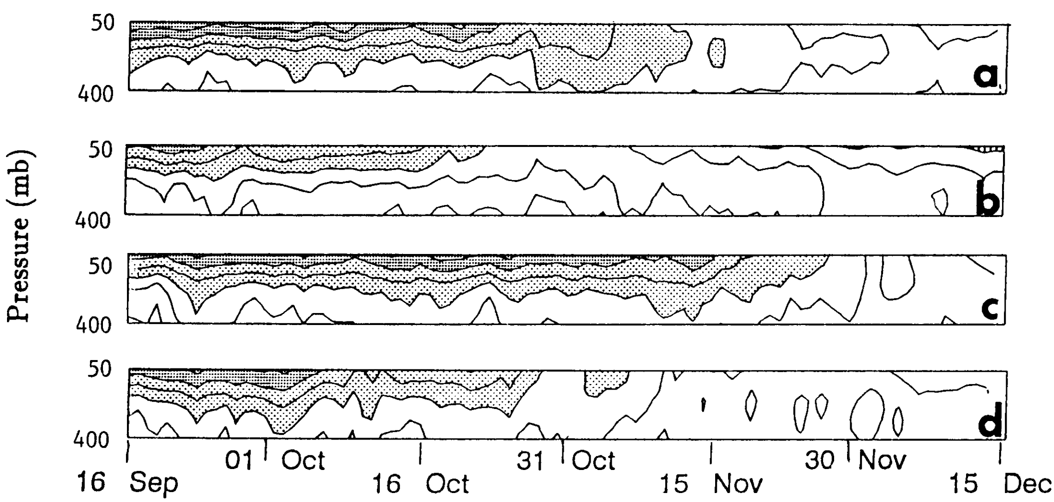

Fig. 1. Vertical (400 mb to 50 mb) time cross-sections of zonally averaged zonal winds at 60° S, contoured every 10 m s^{-1}, with light shade indicating values between 30 and 50 m s^{-1} and heavy shade values larger than 50 m s^{-1}, for 1989 (a), 1988 (b), 1987 (c) and 1986 (d).

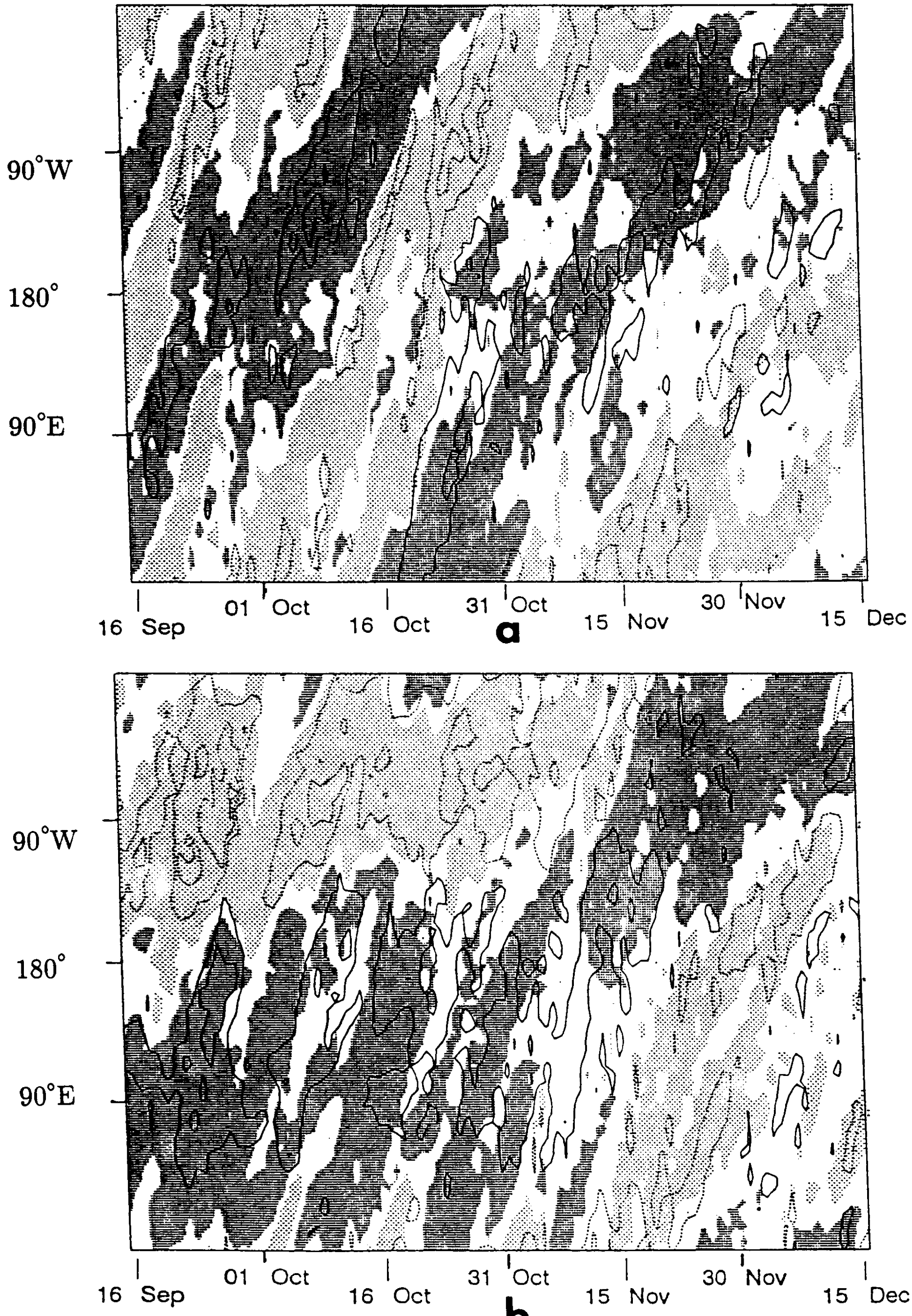

Fig. 2. Longitude-time diagrams of tropopause pressure wave anomalies (deviations from four year spring average) at 60° S contoured every 50 mb for 1986 (a), and 1988 (b). Negative values are dotted and the zero line is omitted. Values of zonally asymmetric ozone anomalies less than −25 DU are shown with light shade and those with more than 25 DU are shown with heavy shade.

the latitude of maximum wave activity during southern spring. Anomalies are defined as differences from the four year average. These anomalies are displayed in Fig. 2 for 1986 and 1988. The figure illustrates the remarkedly different behaviour of atmospheric waves during these 2 years. A stationary wave 1 prevailed during 1988 spring until late October. In contrast, a wave 2 was apparent during the two last weeks of September in 1986, with a period of about 12 days. After this, a propagating wave 1 pattern with a period of 30 to 45 days is evident. Ziemke and Stanford (1990) have discussed oscillations with these periods during southern winter. Fig. 2 also shows a correspondence between low tropopause pressure and low ozone values. The year 1988 is the only year of the four considered in this study to produce a flow reversal to easterlies at 50 mb (Fig. 1) by the end of December. Other years are more similar to the case study of Mechoso et al. (1985) for 1979, which showed westerly flow maintained at lower stratospheric levels.

Correlation coefficients between zonally asymmetric height anomalies at eight pressure levels (50 to 400 mb) and tropopause pressure anomalies are shown in Fig. 3a for the four years separately. This correlation changes sign at about 150 mb for all years with largest values found at 50 mb. This indicates that ridges/troughs at 50 mb are associated with low/high tropopause heights, while the opposite is true at 400 mb. Thus, since high ozone values were found associated with low tropopause heights, ridges at 50 mb are expected to be found in locations with relatively larger values of total ozone. Fig. 3b shows the correlation coefficients between 50 mb heights and heights of other isobaric surfaces. These correlations are about 0.9 between 100 and 50 mb and decline rapidly for higher pressures except for 1987. These results are consistent with an equivalent barotropic structure of stratospheric waves above 100 mb.

Table 1 further quantifies these results by computing the correlation coefficients between planetary waves at 50 mb and 200 mb for the first three waves separately. This is done by expanding the heights at 50 mb (z_1) and 200 mb (z_2) as:

$$z_1(x, t) = S_1(t) \sin kx + C_1(t) \cos kx,$$

$$z_2(x, t) = S_2(t) \sin kx + C_2(t) \cos kx,$$

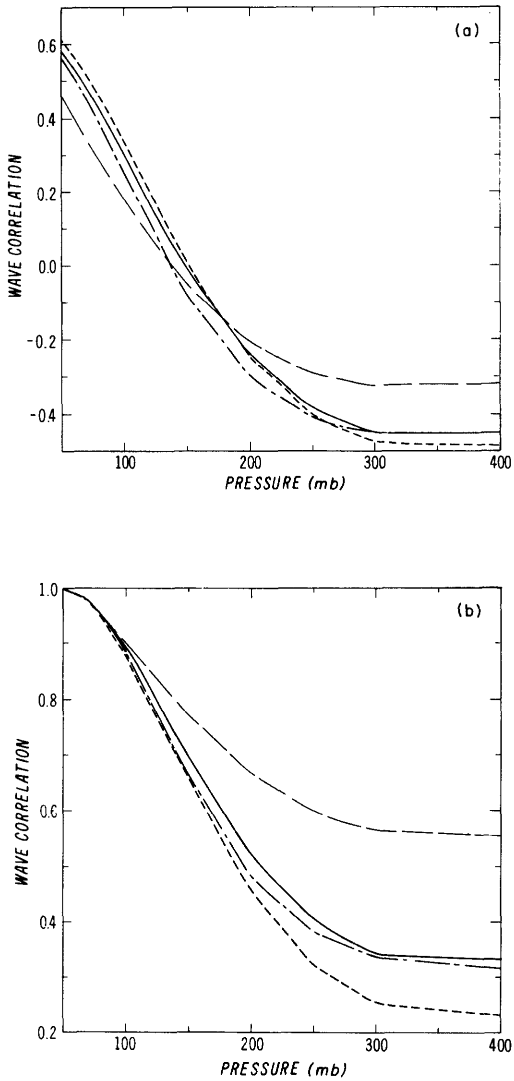

Fig. 3. Correlation height wave anomalies at 50, 70, 100, 200, 250, 300 and 400 mb with tropopause pressure wave anomalies (a) and with 50 mb wave anomalies (b) for 1986 (solid), 1987 (dash), 1988 (small dash) and 1989 (dash dot).

and determining the in-phase ($C(\tau)$) and quadrature ($Q(\tau)$) components as:

$$C(\tau) = (\langle S_1, S_2 \rangle_\tau + \langle C_1, C_2 \rangle_\tau),$$

$$Q(\tau) = (\langle S_1, C_2 \rangle_\tau - \langle S_2, C_1 \rangle_\tau),$$

Table 1. *Planetary wave statistics*

	50 mb heights		Lagged correlations between 50 mb and 200 mb wave components									
Year/ wave#	Average (m)	Standard deviation (m)	$\tau=-2$		$\tau=-1$		$\tau=0$		$\tau=1$		$\tau=2$	
			A	θ	A	θ	A	θ	A	θ	A	θ
1986/1	253	143	0.21	67.3	0.27	48.8	0.33	38.9	0.32	38.2	0.28	39.3
1986/2	197	138	0.29	−2.3	0.47	5.0	0.66*	7.2	0.78*	7.2	0.79*	5.3
1986/3	102	65	0.43	3.0	0.63	3.1	0.81*	3.2	0.77*	2.7	0.59*	2.2
1987/1	216	118	0.54	22.6	0.68*	20.1	0.76*	19.6	0.69*	19.8	0.54	21.2
1987/2	220	108	0.41	0.24	0.56*	3.97	0.70*	4.8	0.74*	3.6	0.70*	1.59
1987/3	109	58	0.30	−1.61	0.53	0.45	0.79*	1.7	0.64*	0.5	0.28	−1.19
1988/1	285	119	0.35	57.6	0.42	44.8	0.47	36.2	0.45	34.2	0.37	37.2
1988/2	137	101	0.36	7.6	0.48	7.7	0.59*	6.5	0.62*	4.9	0.58*	3.5
1988/3	104	69	0.18	7.3	0.59	5.3	0.87*	4.5	0.84*	3.2	0.57*	1.2
1989/1	265	100	0.43	80.2	0.47	70.0	0.53*	61.0	0.54*	59.0	0.53*	5.3
1989/2	197	123	0.53	−3.7	0.62	−0.96	0.71*	0.78	0.70*	0.21	0.58*	−1.2
1989/3	109	62	0.18	2.6	0.47	4.9	0.75*	5.1	0.72*	3.1	0.43	0.14

A and θ are the coherence and phase between 50 mb and 200 mb wave components (see text for definitions).
* Significant at the 95% level.
Positive lag τ indicates that the stratosphere lags.

where the lagged correlation coefficient $\langle A, B\rangle_\tau$ at lag τ is defined as:

$$\langle A, B\rangle_\tau = \frac{1}{N-\tau}\sum_{i=1}^{N-\tau} A(i)\,B(i+\tau)/\sigma_A\sigma_B,$$

and where σ_A and σ_B are the standard deviations of A and B, respectively. The correlation coherence $A(\tau)$ and phase lag $\theta(\tau)$ are then obtained as:

$$A(\tau) = (C^2(\tau) + Q^2(\tau))^{1/2},$$

$$\theta(\tau) = \tan^{-1}(-Q(\tau)/C(\tau)).$$

The 95% significance level is estimated using the procedure outlined by Randel (1987b). The average intensity of wave 1 at 50 mb (first column Table 1) is larger than those of waves 2 and 3 for all years except 1987 when the wave 2 component was the largest. Comparable values of standard deviations of wave 1 and 2 intensity for all year results from the slower propagation speed of wave 1 than wave 2. During 1988, wave 1 is more than twice as strong as wave 2. After 1986 the first two waves time variability (described by the standard deviation of wave intensity) decreased. These results are consistent with those of Manney et al. (1991) who also documented the existence of wave 2 during late southern winter and early spring.

Lagged correlations between 50 and 200 mb are useful to identify vertically propagating waves. A positive phase between 50 and 200 mb at $\tau=0$ indicates a westward tilt with height. Results for wave 1 are only statistically significant for 1987, when this wave showed a very small vertical tilt with height, and for 1989, when a westward tilt of 61° is observed between 200 and 50 mb indicating upward energy propagation. Waves 2 and 3 are significantly correlated at both levels, but with no phase shift. This indicates a dominant barotropic structure for wave 1 during 1987 and waves 2 and 3 for all years. We note that the standard deviations of the first two waves are comparable in magnitude while the averaged intensity of wave 2 over the four springs is about 75% of that of wave 1. Fig. 2 and the correlations shown in Fig. 3a indicate that low ozone values are expected in 50 mb troughs and high ozone values in 50 mb ridges. These relationships are quantified next using empirical orthogonal functions (EOF) for total ozone and 50 mb heights. EOF analysis is preferable to the one-dimensional Fourier representation used in this section since it describes the two-dimensional pattern that explains most of the total variance. The wave decomposition presented above was done at a single latitude and it did not permit identification of the meridional wave structure. Also, the first EOF represents the most commonly observed pattern, with successive EOFs contributing increasingly less to the total variance. This is not the case with wave components.

3. EOF Analyses

3.1. Methodology

The large interannual variability of the 4 years chosen for study complicates interpretation of EOF patterns based on the four austral springs. Therefore, we opted to compute the EOF's for each year separately, and to use the resulting structures to describe the dominant patterns of

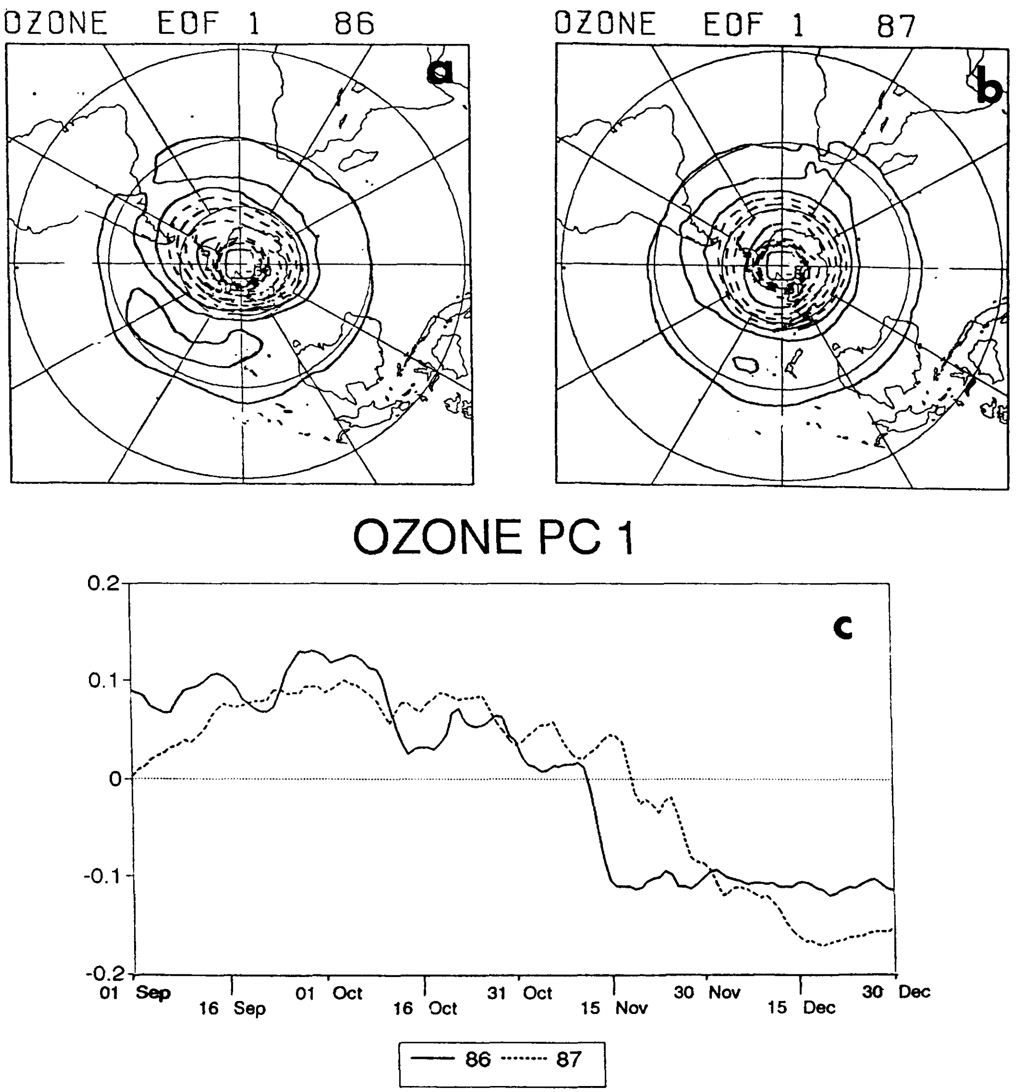

Fig. 4. First empirical orthogonal function (EOF) representing the seasonal trend of ozone, normalized to unit length × 10, contour interval 15, for 1986 (a) and 1987 (b) which explain 33.6% and 43.1% of the total variance, respectively. Negative values are dashed. Time series of the associated principal component (PC) is shown in (c).

horizontal variability for the different years. The horizontal domain extends from 30° S to 80° S for a 5° by 5° latitude-longitude grid. Covariances were area weighted. The EOF analysis is done on the difference of daily values from the seasonal time average) of total ozone and of zonally asymmetric heights. Certain pairs of EOF patterns are in quadrature with each other representing oscillations.

3.2. Results

The EOF analyses reveal three different pattern types. These describe the seasonal trend, a quasi-stationary or eastward propagating wave 1 with a period of 25 to 45 days and a fast moving wave 2 with a period of 10 to 15 days. These patterns are consistent with the results described above at 60° S. Wave amplitudes maximize at about 60° S with meridional half wavelengths of 30° latitude.

3.2.1. Seasonal trend. Fig. 4 shows the first EOF for 1986 and 1987 which explains 33.6% and 43.1%, respectively, of the total ozone variance. The patterns are similar with low polar values and positive loadings at mid-latitudes. These are nearly zonally symmetric, with an almost linear decay from September to October as indicated by the PC. The meridional gradient reverses sign during November with a linear trend again until the end of December. The time evolution of the seasonal change is quite different for these two years, with most of the seasonal change in 1986 (a normal year) taking place with a phase shift over a 5–10 day period, while for 1987 the transition to summer is slow and the trend downward continues until late December. The seasonal evolution of the zonally symmetric height field (not shown) replicates closely the zonally symmetric ozone distribution. This pattern does not appear in our EOF analyses which are conducted only in the zonally asymmetric height component. Total ozone PC 1 changes sign on November 10 (day 71) and November 20 for 1986 and 1987, respectively. These are the approximate dates for the zonally averaged zonal wind (Fig. 1) to decrease to about 50% of its spring maximum.

Similar trends are also found in 1988 and 1989 (Fig. 5) with one notable exception. The seasonal trend of the same EOF pattern are now well correlated with zonally asymmetric wave patterns which tend to displace the vortex from its central polar position. Correlation coefficients between ozone and height PCs are 0.96 and 0.94, respectively, for 1988 and 1989. It is of interest that the large height gradients in the eastern hemisphere have no counterpart on the ozone configuration. Nevertheless, the high correlation coefficients between corresponding PCs suggest the role of anticyclonic anomalies in mixing regions with high ozone values between 30 and 60° S. Note that this is not the case for the ozone depleted region which exhibits strong radial gradients.

3.2.2. Wave 1 pattern. The next EOF patterns are shown in Figs. 6 through 9 for the years 1986 through 1989. These generally exhibit a wave 1 pattern. During 1986 (Fig. 6) both ozone and height patterns describe a traveling wave, with a period of 36 days. This is apparent in the time series (Figs. 6e, f) that show the propagation of the two components which are in quadrature with each other. The correlation coefficient between EOF 2 for ozone and EOF 1 for 50 mb heights is −0.81. Figs. 6a, c, g and this negative correlation coefficient indicates that when a center of high total ozone is located close to 0° E (as on October 20) a center of maximum 50-mb heights is found approximately at 45° W. This phase difference implies a vertically tilting height wave. The total ozone distribution expected from a wave with no tilt in the vertical is presented in the Appendix. This linear wave model assumes an equivalent barotropic wave (between 5 and 150 mb) embedded in a zonal flow constant with height. The 5 to 150 mb layer constitutes about half of the stratosphere thickness (by mass) and it is centered at the height of maximum ozone density. Using the standard atmosphere profile for ozone density, the vertically averaged ozone contributed by this layer is 384 DU (A11). Furthermore, the amplitude of the wave is steady in time with no appreciable amplification or decay. This model is similar to that used by Schoeberl and Krueger (1983) for medium-scale waves which are trapped in the troposphere. The main conclusion is that total ozone and height patterns exhibit the same functional dependence in the horizontal domain (A4 and A13). The EOF analysis gives a value of 100 DU for the amplitude of the ozone wave, while the linear model predicts a value of 123 DU for a zonal wind ($\bar{u}$) of 20 m/s. Ozone and wave 1 heights for 1986 differ from the model assumptions in some important aspects. First, the wave does not exhibit an equivalent barotropic structure as

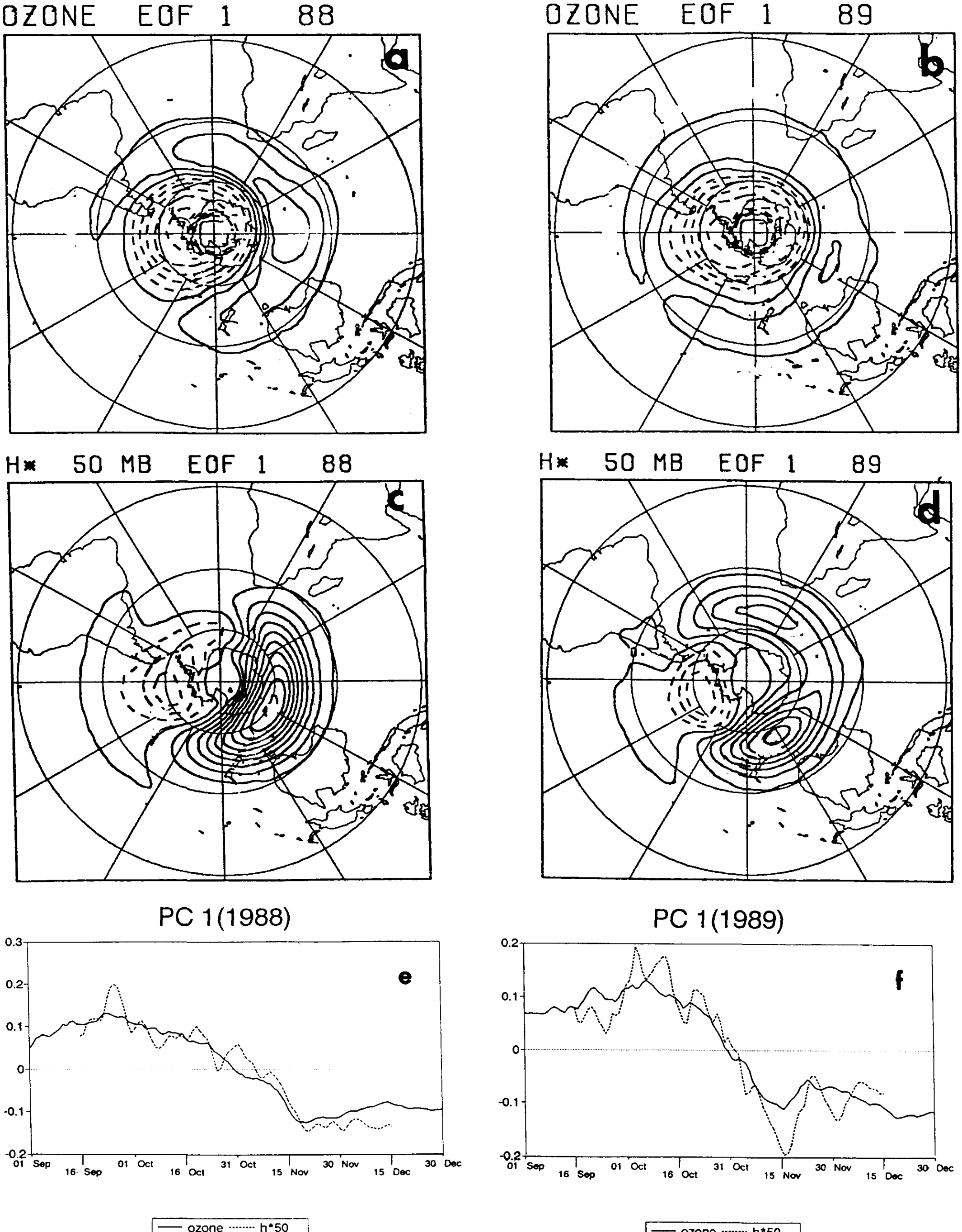

Fig. 5. Same as Fig. 4, but for the first EOF of ozone for 1988 (a) and 1989 (b) and of 50 mb heights, normalized to unit length × 100, contour interval 4, for 1988 (c) and 1989 (d), representing 47%, 39%, 54% and 31% of the total variance, respectively. Negative values are dashed. Time series of principal components are shown in (e) and (f).

indicated by Table 1. The table indicates a phase difference of 39° between 50 and 200 mb, also suggesting vertical propagation. If we consider this vertical tilt (approximately 40°/10 km) to hold between 50 and 5 mb, a phase shift of about 90° is obtained between 150 and 5 mb. Such shifts would cause the total ozone pattern to be shifted with respect to that of the height field. Coherence values indicate that this result is not statistically significant for the three month period. This is not surprising considering that this wave event only lasted about one month (one third of the seasonal record). Second, the wave is not steady; there is a burst of wave energy about 20 October which produces considerable amplification of the wave. This, in conjunction with the observed longitudinal lag between the total ozone and 50 mb heights suggests vertical propagation and tilting of waves with height.

The year 1987 (Figs. 7, 10) is different from

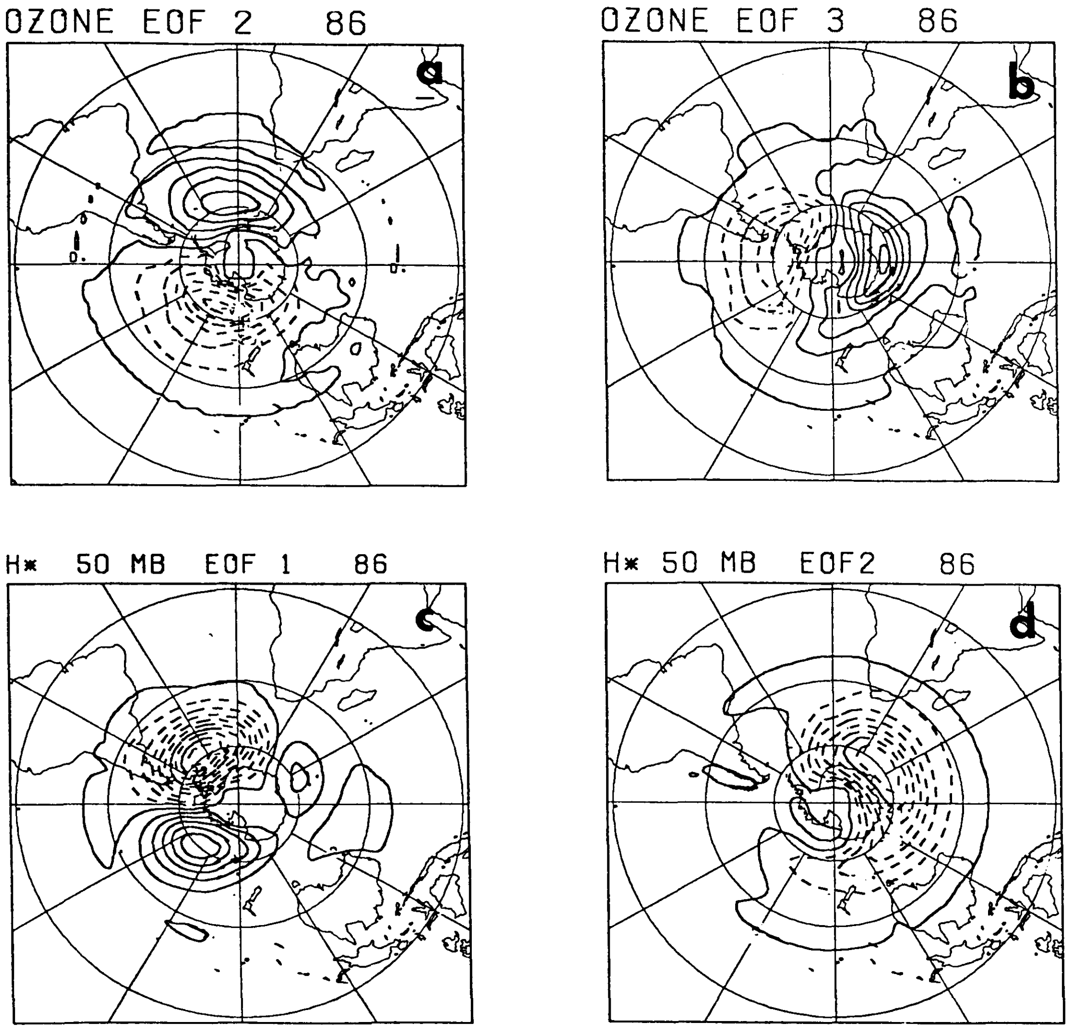

Fig. 6. Same as Fig. 5 but for 1986 EOFs as indicated in the figure, which exhibit dominant wave 1 patterns. The normalized ozone EOFs are contoured every 10. These represent 17.4% (a), 13.5% (b), 29.6% (c) and 26.7% (d) of the total variance. Negative values are dashed. Time series of principal components are shown in (e), (f) and (g).

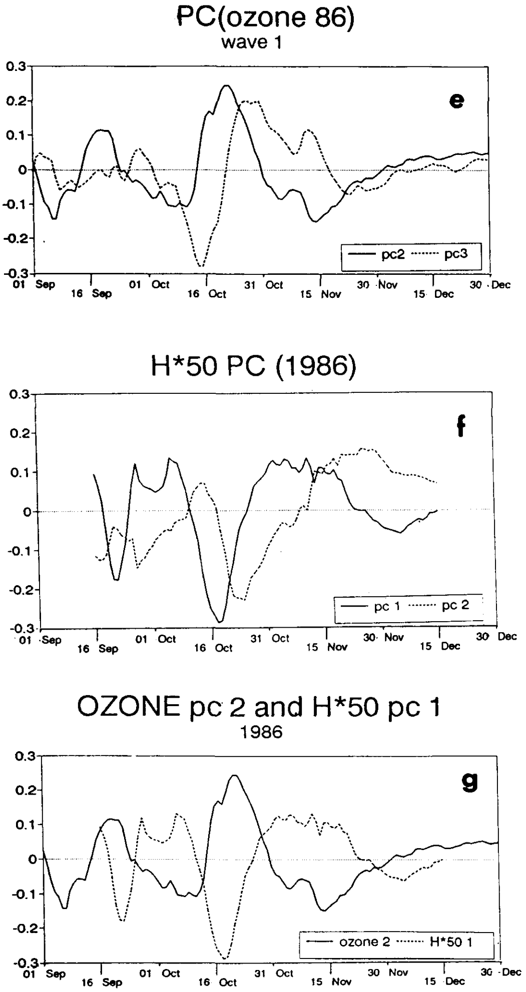

Fig. 6. Continued.

the other four years. There is no well defined wave 1 among the first four leading EOFs for the height field. The largest wave 1 components are found for the ozone EOF 2 and the 50 mb height EOF 1 (Figs. 7a and b). The correlation coefficient between the two principal components is 0.75, with the two time series mostly in phase (Fig. 7e). Table 2 summarizes the main characteristics of the wave patterns as obtained from the EOF analysis. The year 1987 more closely agrees with the assumptions of the linearized wave model than 1986. At 60° S the ozone EOF 2 patterns exhibits maximum values of about 100 DU on October 15. An estimate of the period may be obtained from the height PCs for EOF 1 and 2 and gives $(\bar{u} - c) = 10$ m/s. A value of 20 m/s is taken for $\bar{u}$ as representative of the zonally averaged October value between 12 to 32 km. With these values, the amplitude of meridional and vertical advections (A12) are about the same. Eqs. (A3) and (A12) may be combined to estimate the amplitude of the total ozone wave. This value is 140 DU, a 40% overestimate of the observed value.

EOFs for 1988 are shown in Fig. 8. The ozone field has more of a wave 1 structure than the height field, but both PCs evolve approximately in phase during October and November. The time series reflect the prevailing quasi-stationary character of this pattern from mid-October to mid-November with considerable amplification and decay before and after this period, respectively. The observed total ozone amplitude, as given by the EOF analysis), during this period is about 90 DU. The linear wave model of the Appendix predicts an amplitude of 111 DU for a basic state zonal wind $(\bar{u})$ of 18 m/s. The correlation coefficient between the ozone and height PCs is 0.8. On approximately 15 November the principal component changes sign indicating a 180° longitude pattern shift. After this date, the total ozone wave 1 starts moving eastward (Fig. 2).

The year 1989 exhibits the highest correlation coefficient between the ozone and 50 mb height patterns (Fig. 9). The correlation coefficients between ozone and 50 mb heights for EOF 2/EOF 3 are 0.93/0.84, respectively. From mid-October to mid-November the amplitude of the wave is approximately steady and propagates eastward with a speed of about 10 m/s. The basic state zonal wind $(\bar{u})$ is taken as 15 m/s. The ozone amplitude (estimated from Fig. 9) is approximately 120 DU. Eqs. (A3) and (A12) predict a value of 210 DU for the amplitude of the ozone wave, an overestimate by about a factor of 2. An overestimate by the equivalent barotropic wave model is expected for the case of vertically tilting waves. Table 1 indicates a shift of 61° between 200 and 50 mb this year. This is also confirmed by the longitudinal phase shifts of the heights and total ozone EOFs.

3.2.3. Wave 2 pattern. Higher EOFs exhibit similar wave 2 structure for all years and they explain, in general, a small fraction of the variance. The contributions from the next two ozone EOFs explain 9%, 12%, 8.4%, and 8.7% of the

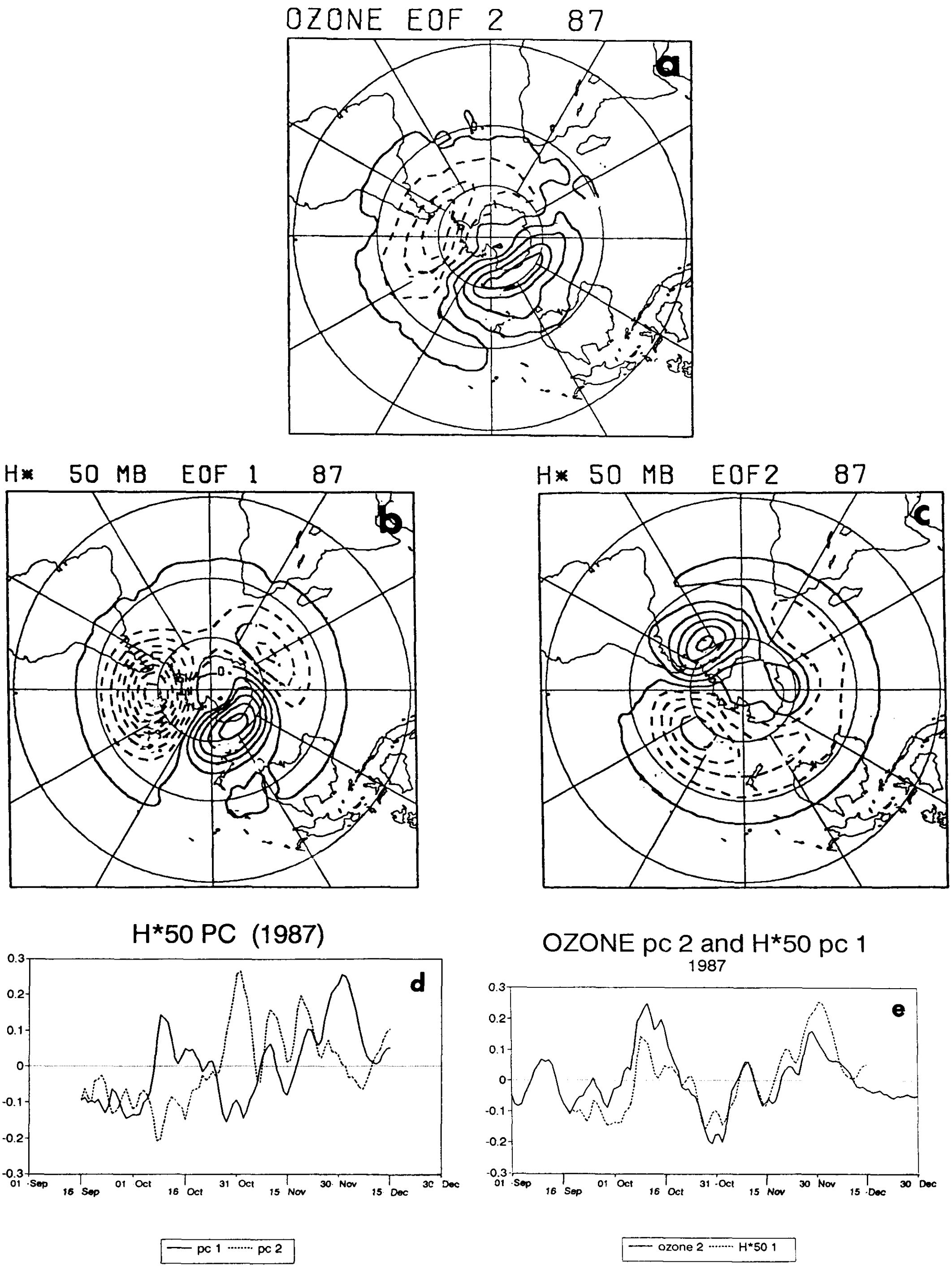

Fig. 7. Same as Fig. 6 but for 1987 EOFs representing 14% (a) 33% (b) and 17% (c) of the total variance. Time series of principal components are shown in (d) and (e).

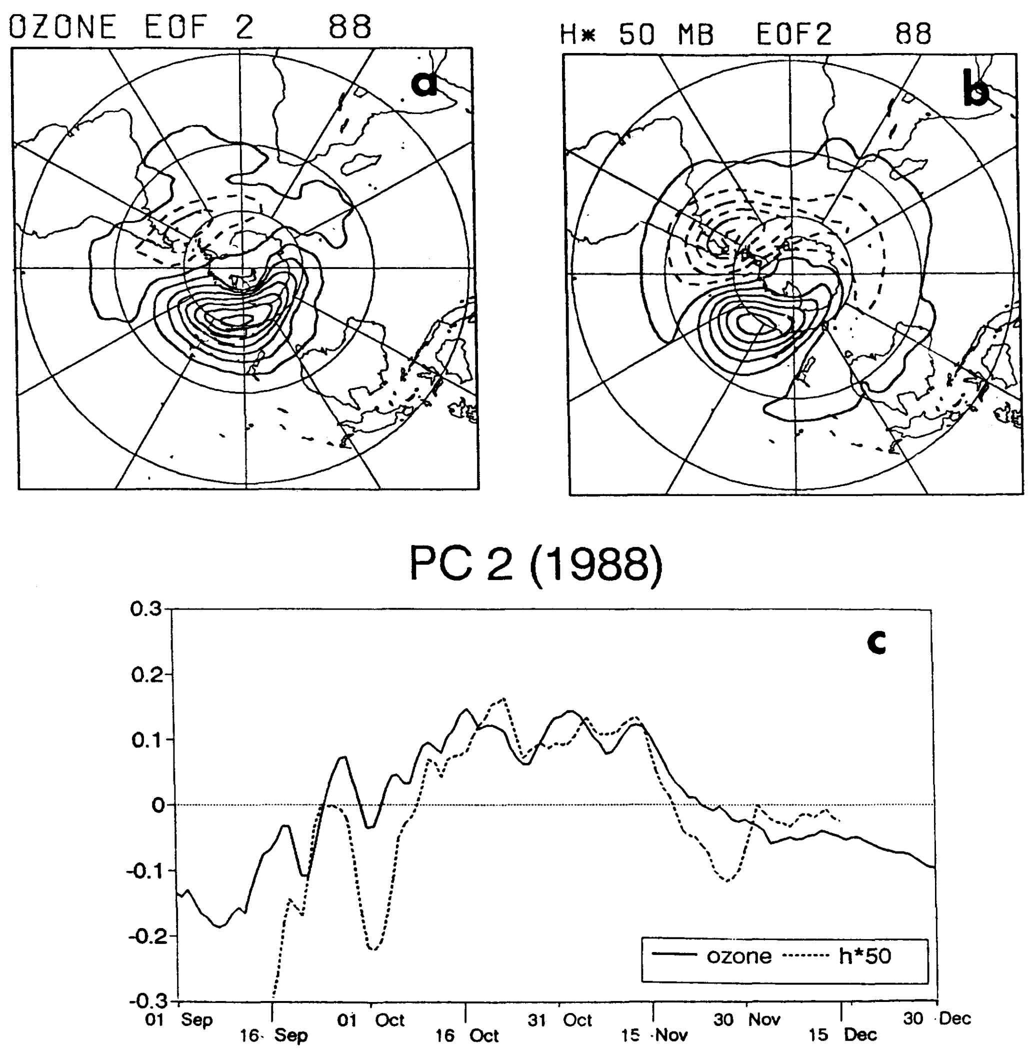

Fig. 8. Same as Fig. 6 but for the second EOF for 1988 representing 17.2% (a) and 17.7% (b) of the total variance. Time series of principal components are shown in (c).

variance for years 1986 through 1989, and 7.4%, 25%, 12.2% and 12.5% of the height variance for the same years. These values are small for all years except 1987. Therefore, only the 1987 EOFs and PCs are shown in Fig. 10. The ozone patterns are in quadrature with each other representing eastward propagating oscillations with a speed of about 10 m/s. This is the only year for the period of study in which traveling wave 2 is as strong as wave 1. Correlation coefficients between the ozone and 50 mb heights for PC 3 and 4 are 0.77 and 0.79, respectively. Wave amplitude is about 70 DU. Eqs. (A3) and (A14) predict the ozone wave amplitude to be 53 DU for an average zonal wind of 20 m/s, somewhat underestimating the observed value. The longitudinal shift between the ozone and height pattern suggests that there is some vertical tilt to the height wave. In that case, an overestimate rather than an underestimate by the linear barotropic model is expected. After 1 December there is an amplification of the height wave, while the ozone wave decreases in

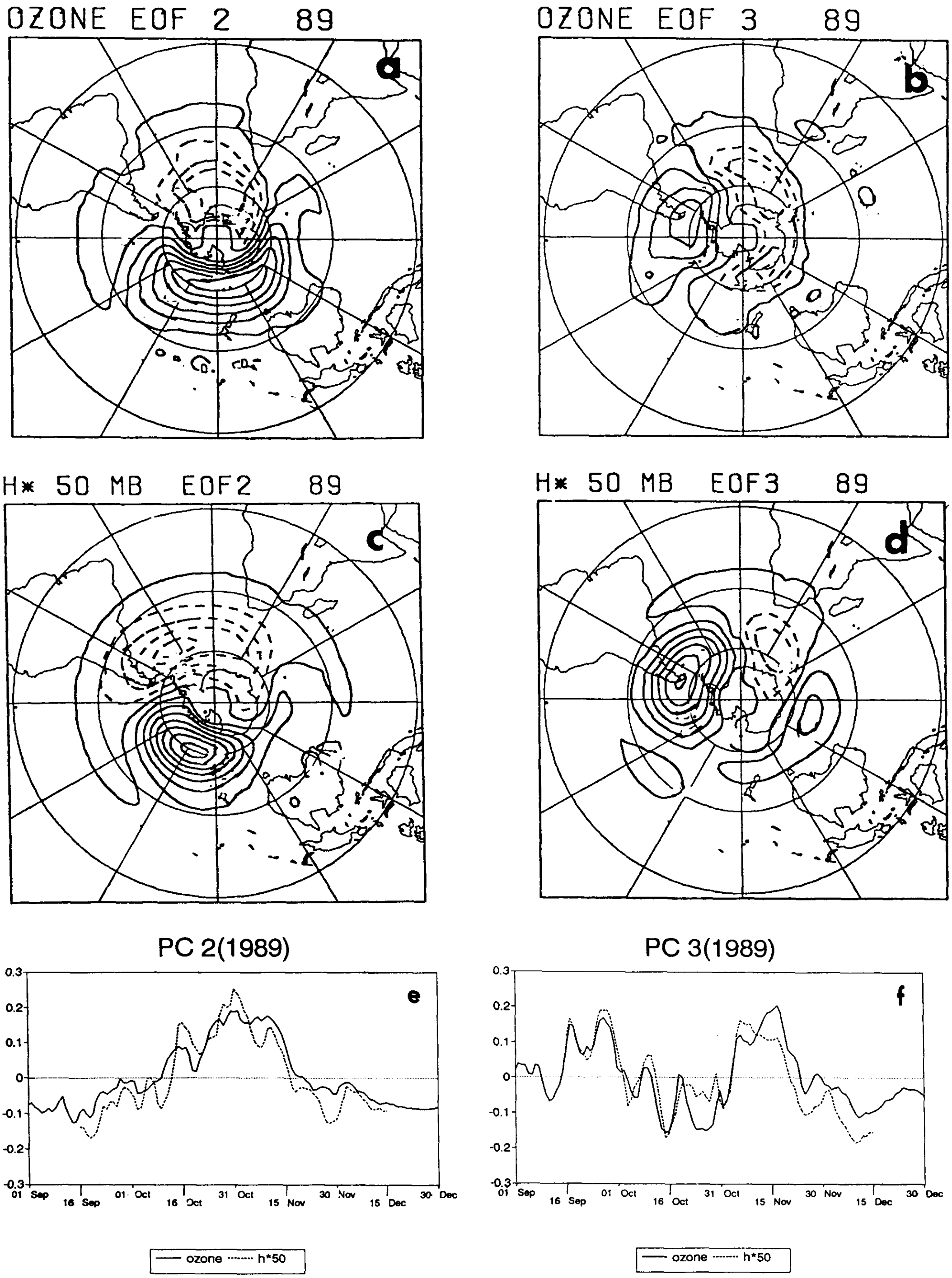

Fig. 9. Same as Fig. 6 but for 1989 EOFs, representing 21%, 7%, 24% and 16% of the total variance. Negative values are dashed. Time series of principal components are shown in (e) and (f).

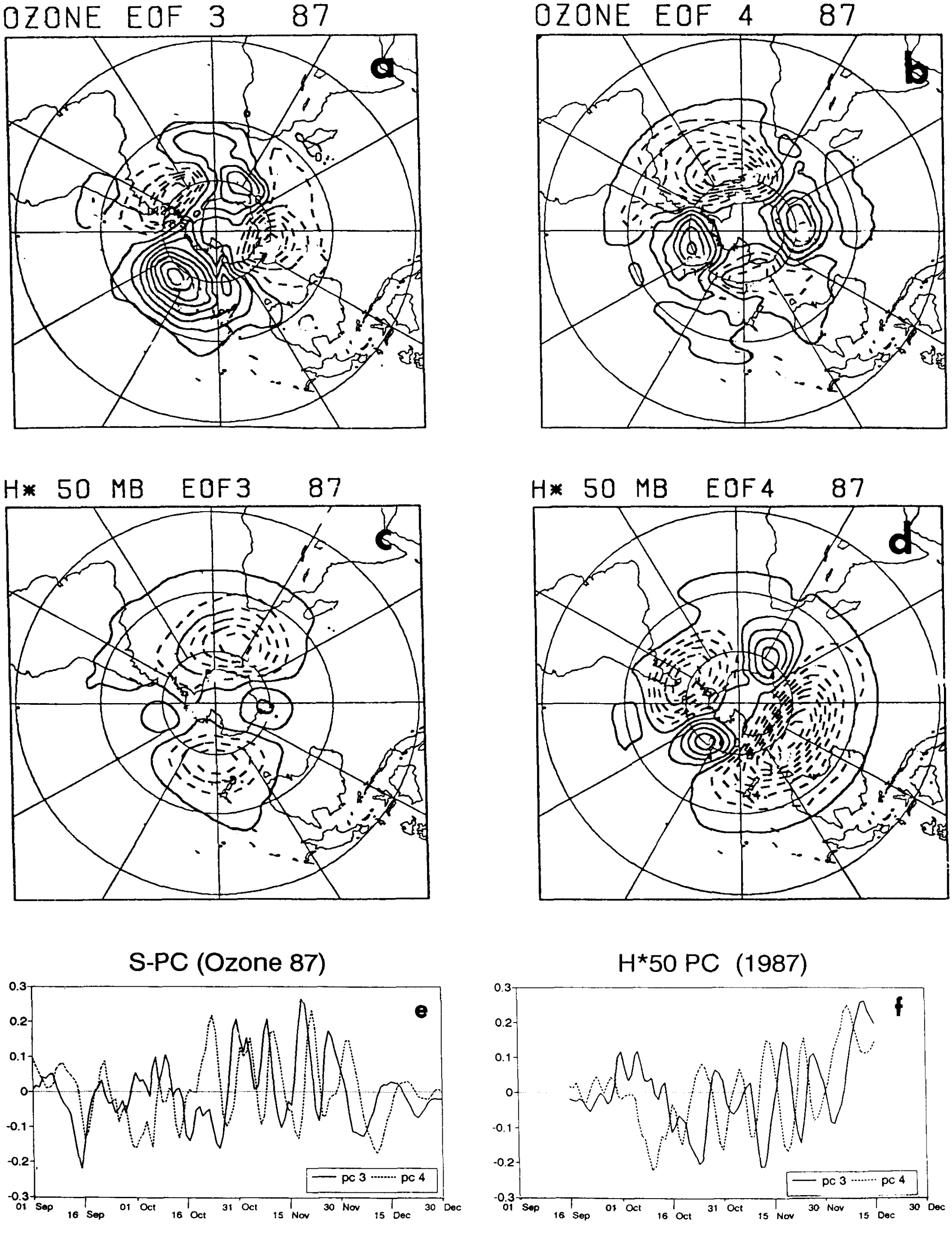

Fig. 10. 1987 normalized EOF 3 and EOF 4 for ozone and 50 mb heights, contour interval 5 for ozone, 4 for heights. These exhibit wave 2 patterns and represent 6.5% (a), 5.9% (b), 13.2% (c) and 11.5% (d) of the total variance. Negative values are dashed. Time series of principal components are shown in (e) and (f).

Table 2. *Summary of EOF's characteristics for waves 1 and 2*

		Total ozone and 50 mb height phase lags	Eastward propagation?	Steady amplitude in 50 mb waves?
EOF wave 1	1986	Ozone leads by $\frac{1}{2}\pi$ (upper half of map)	yes	no (strong amplification in mid-October)
	1987	in phase	yes	yes (during November)
	1988	in phase	no	yes (mid-October to mid-November)
	1989	ozone leads by $\frac{1}{2}\pi$ (upper half of map)	yes	no (strong amplification through mid-October) yes (mid-October through mid-November)
EOF wave 2	1986	in phase	yes	yes (through mid-November)
	1987	ozone lags by $\frac{1}{2}\pi$	yes	no (through mid-October) yes (mid-October–mid-November)
	1988	in phase	yes	yes (late September–early October) no (after mid-October)
	1989	in phase	yes	no (amplitude peaks 9/20 and 10/20)

magnitude. This occurs at the time of substantial decrease in the strength of the polar vortex and indicates that the ozone waves are now being filled and ozone gradients are weakened.

Though the EOF patterns and PC for wave 2 during the other three years are not shown, Table 2 summarizes their general characteristics. Observed average amplitude for these three years are 60 DU, 40 DU, and 60 DU for the years 1986, 88 and 89. These waves propagate eastward with an average speed of 10 m/s as during 1987. Eqs. (A3) and (A14) predict the amplitude for the ozone wave to be 53 DU which is quite close to the observed values. For all wave 2 patterns vertical advections are of same magnitude and reinforce meridional advections. All of the leading EOFs shown here for the years 1986 through 1989 depict high correlation coefficients between the ozone and 50 mb height PCs during spring, indicating the feasibility of basing forecasts of ozone content on 50 mb height predictions. These results are probably due to the weak amplitude of Southern Hemisphere waves, which do not actively mix the air within the polar low with that outside the polar low during spring. The high relationships between the ozone and 50 mb height waves are not expected to exhibit similar relationship during boreal spring, where active planetary waves cause the quick erosion and mixing of the winter vortex.

4. Summary and conclusions

The relationship between ozone concentration and tropospheric synoptic waves, particularly for the Northern Hemisphere, have been known for many decades (e.g., Reed, 1950). Nevertheless, no statistical quantification of hemispheric stratospheric height waves and total ozone content patterns has been done in the past, partly due to the lack of reliable daily stratospheric analyses. Our present goal is to present such quantification for the spring transition in the Southern Hemisphere. The main results are as follows.

• The leading EOFs for both the ozone and 50 mb heights wave exhibit wave 1 and 2 patterns. These patterns are highly correlated, with high/low ozone values associated with ridges/troughs in the height field. This is due to the colocation in longitude of lower stratospheric ridges/troughs with low/high tropopause altitudes, while the opposite is true for the upper troposphere where troughs in the height field have low tropopauses. An equivalent barotropic linear wave model between 5 and 150 mb is used as a framework to explain the high correlations between ozone and 50 mb height waves. The height wave is embedded on a zonally averaged total ozone profile with maximum values at mid-latitude and decreasing values towards the south pole. Such model is found to approximate the observed EOF total ozone wave 1 amplitude (of approximately 100 DU) and that of wave 2 (of approximately 60 DU) within 40% of the observed value for all years, except for the 1989 wave 1. That year was characterized by a wave 1 in the height field which tilted westward with height. The barotropic wave model over-estimated the ozone wave amplitude by almost a factor of 2. This is expected since the vertical tilt causes changes in the sign of meridional ozone advection with altitude and results in the vertically integrated ozone density to be less than what would be predicted by a height wave with no vertical tilt.

- The leading EOF of the ozone distribution consists of a seasonal trend which represents about 40% of the variance. It has negative loadings centered over the South pole and positive loadings in midlatitudes. For the years 1988 and 1989, this EOF exhibits a high correlation with a wave 1 in 50 mb heights.
- The wave 1 is usually centered at 60–65°S and explains about 40 to 55% of the height variance. It exhibits eastward propagation with periods of 30 days or longer (1986, 87, 89) or it is quasi-stationary (1988). This wave is weak during 1987, a year with low ozone values which persisted into summer.
- The wave 2 patterns represents about 8% of the ozone variance and 12–25% of the height variance. It is an eastward traveling disturbance with period of 10–12 days. It is best defined while the polar vortex is strong and the ozone wave amplitude decays sharply after onset of the summer regime. Similar behaviour is found for the 50 mb height wave 2, except for 1987 when the amplitude of the wave increased after 1 December.

5. Acknowledgements

The reviewer's comments were very helpful to improve this manuscript and are gratefully acknowledged. This investigation was supported by NASA grant NAG-527 and NSF grant ATM 9114073 to the University of Utah and by USAF/AWS support to K. Callahan. The ozone data was kindly provided by the Ozone Processing Team of NASA/Goddard Space Flight Center.

6. Appendix

Linear analysis of total ozone waves

Conservation of ozone mixing ratio concentration is described by

$$\frac{d\mu}{dt}=0,$$

$$\frac{d\mu}{dt}=\frac{\partial\mu'}{\partial t}+\bar{u}\frac{\partial\mu'}{\partial x}+v'\frac{\partial\bar{u}}{\partial y}+w'\frac{\partial\bar{\mu}}{\partial p}=0, \qquad \text{(A1)}$$

where $\mu=\bar{\mu}+\mu'$; $(\bar{\ })$ denotes a zonal average, $(\ )'$ the deviation from the zonal average, u and v are zonal and meridional wind components and $w=dp/dt$. Multiply (A1) by ρ and integrate between z_T and z_B,

$$\int_{z_B}^{z_T}\rho\frac{\partial\mu'}{\partial t}dz+\int_{z_B}^{z_T}\rho\bar{u}\frac{\partial\mu'}{\partial x}dz+\int_{z_B}^{z_T}\rho v'\frac{\partial\bar{\mu}}{\partial y}dz+\int_{z_B}^{z_T}\rho w'\frac{\partial\bar{\mu}}{\partial p}dz=0$$

substitute from the hydrostatic equation and rearrange,

$$\frac{\partial}{\partial t}\int_{p_T}^{p_B}\mu'\,dp=-\bar{u}\frac{\partial}{\partial x}\int_{p_T}^{p_B}\mu'\,dp-\int_{p_T}^{p_B}v'\frac{\partial\bar{\mu}}{\partial y}dp-\int_{p_T}^{p_B}w'\frac{\partial\bar{\mu}}{\partial p}dp. \qquad \text{(A2)}$$

Define the perturbation total column ozone,

$$TO'\equiv\int_{z_B}^{z_T}\rho\mu'\,dz=\frac{1}{g}\int_{p_T}^{p_B}\mu'\,dp$$

and substitute into (A2),

$$\frac{\partial TO'}{\partial t}+\bar{u}\frac{\partial TO'}{\partial x}=-\underbrace{\frac{1}{g}\int_{p_T}^{p_B}v'\frac{\partial\bar{\mu}}{\partial y}dp}_{(A)}-\underbrace{\frac{1}{g}\int_{p_T}^{p_B}w'\frac{\partial\bar{\mu}}{\partial p}dp}_{(B)}. \qquad \text{(A3)}$$

From the thermodynamic energy equation linearized about a basic state constant with height:

$$w' = \frac{1}{\sigma}\left(\frac{\partial}{\partial t} + \bar{u}\frac{\partial}{\partial x}\right)\left(-\frac{\partial \phi'}{\partial p}\right)$$

where

$$\sigma = -\frac{\alpha}{\theta}\frac{\partial \theta}{\partial p} = \frac{H^2}{p^2} N^2.$$

$H = 6378$ m is the e-folding height for an isothermal stratosphere of 218°K. N^2 is approximately constant in the stratosphere and has a typical value of $4.0 \times 10^{-4}\ \mathrm{s}^{-2}$. Geopotential waves with no vertical tilt are described by

$$\phi' = \hat{\phi}(p) \sin k(x - ct) \cos Wy. \tag{A4}$$

The change of geopotential wave amplitude with pressure is approximated by

$$\frac{\partial \hat{\phi}(p)}{\partial \ln p} \approx -RT^* \approx -3200\ \mathrm{m^2\,s^{-2}} \quad \text{at} \quad 60°\mathrm{S}, \tag{A5}$$

consistent with the wave 1 amplitude change between 50 mb and 200 mb for the years of this study. R is the gas constant for dry air. Then:

$$w' = \frac{RT^* k}{N^2 H^2} (\bar{u} - c)\, p \cos k(x - ct) \cos Wy, \tag{A6}$$

$$v' = \frac{\hat{\phi}(p)}{f_0} k \cos k(x - ct) \cos Wy, \tag{A7}$$

where f_0 is the coriolis parameter. Furthermore, we assume that

$$\overline{\rho\mu} = \widetilde{\rho\mu}(p)\, Y(y). \tag{A8}$$

The vertical profile of ozone concentration maximizes at about 22 km with a maximum value of about $8 \times 10^{18}\ \mathrm{m}^{-3}$. We approximate the vertical profile for the ozone density (U.S. Standard Atmosphere, 1976) between p_T and p_B by:

$$\frac{\partial \widetilde{\rho\mu}}{\partial \ln p} = b, \qquad p_\mathrm{T} \leqslant p < p_\mathrm{M},$$
$$\frac{\partial \widetilde{\rho\mu}}{\partial \ln p} = -b, \qquad p_\mathrm{M} < p \leqslant p_\mathrm{B}, \tag{A9}$$

where p_M = atmospheric pressure at the level of maximum ozone density and

$$b = \frac{\widetilde{\rho\mu}(p_\mathrm{M}) - \widetilde{\rho\mu}(p_\mathrm{T})}{\ln(p_\mathrm{M}/p_\mathrm{T})},$$

with

$$p_\mathrm{T} \approx 5\ \mathrm{mb}\ (32\ \mathrm{km}) \quad \text{and} \quad p_\mathrm{B} \approx 150\ \mathrm{mb}\ (12\ \mathrm{km}),$$
$$\widetilde{\rho\mu}(p_\mathrm{T}) \approx \widetilde{\rho\mu}(p_\mathrm{B}) \approx \tfrac{1}{4}\widetilde{\rho\mu}(p_\mathrm{M}). \tag{A10}$$

With these values

$$\frac{1}{g}\int_{p_T}^{p_B} \mu\, \mathrm{d}p = 10^{23}\ \text{molecules}\ \mathrm{m}^{-2} \approx 384\ DU. \tag{A11}$$

The average meridional variation of zonally averaged ozone can be estimated from Figs. 4 and 5 to be 100 DU over 20° latitude with a maximum at mid-latitudes. This gives a value for

$$\frac{\partial Y}{\partial y} = 1.2 \times 10^{-7}\ \mathrm{m}^{-1}.$$

With these assumptions (A) and (B) with wavenumber k for wave 1 are

$$(A) = 214 \times 10^{-6} \cos k(x - ct) \times \cos Wy (DU/s),$$
$$(B) = 23 \times 10^{-6} (\bar{u} - c) \cos k(x - ct) \times \cos Wy (DU/s). \tag{A12}$$

Eqs. (A6) and (A7) indicate that meridional and vertical motions are in phase. Northerlies ($v' < 0$) cause a local increase in TO' (A3) advecting the ozone rich air of mid-latitudes. The associated sinking motion ($w' < 0$) reinforces this increase by advecting air with high ozone mixing ratio from higher levels. With $\bar{u} - c \approx 10$ m/s, both the meridional and vertical advections are of the same magnitude. This is the same conclusion as reached by Schoeberl and Krueger (1983) for the case of medium scale waves. This agreement is expected, since the stratospheric planetary waves considered here exhibit, in general, no vertical tilt in the lower stratosphere where the advection of ozone is largest. For late spring when $\bar{u}$ decreases, or for faster moving waves, the meridional advection is dominant.

It also follows from (A3) and (A12) that:

$$TO' = \widehat{TO} \sin k(x-ct) \cos Wy, \tag{A13}$$

with the ozone and height field in phase. The four year average intensity of wave 2 (see Table 1) is about 75% of that of wave 1. The resulting meridional and vertical advection for wave 2 are:

$$\begin{aligned}(A) &= 160 \times 10^{-6} \cos 2k(x-ct) \\ &\quad \times \cos Wy(DU/s), \\ (B) &= 17 \times 10^{-6}(\bar{u}-c) \cos 2k(x-ct) \\ &\quad \times \cos Wy(DU/s).\end{aligned} \tag{A14}$$

REFERENCES

Andrews, D. G., Holton, J. R. and Leovy, C. B. 1987. *Middle atmosphere dynamics*, (eds. R. Dmowska and J. R. Holton). Academic Press. 489 pp.

Beasley, D. 1991. News and Notes. *Bullet. Amer. Met. Soc. 72*, 1949–1950.

Bowman, K. P. and Krueger, A. J. 1985. A global climatology of total ozone from the Nimbus 7 total ozone mapping spectrometer. *J. Geophys. Res. 90*, 7967–7976.

Mahlman, J. D., Levy, H. and Moxim, W. J. 1980. Three-dimensional tracer structure and behaviour as simulated in two ozone precursors experiments. *J. Atmos. Sci. 37*, 655–685.

Manney, G. L., Farrara, J. D. and Mechoso, C. R. 1991. The behaviour of wave 2 in the Southern Hemisphere stratosphere during late winter and early spring. *J. Atmos. Sci. 48*, 976–998.

McPeters, R. D. and the NASA Ozone Processing Team. 1990. Results of calibration of Nimbus 7 TOMS Ozone data using the pair justification technique. In: *Digest of topical meeting on optical remote sensing of the atmosphere, vol. 4*, pp. 413–416.

Mechoso, C. R., Yamazaki, K., Kitoh, A. and Arakawa, A. 1985. Numerical forecasts of stratospheric warming events during the winter of 1979. *Mon. Wea. Rev. 113*, 1015–1029.

Meetham, A. R. 1937. The correlation of the amount of ozone with other characteristics of the atmosphere. *Quart. Jour. Roy. Met. Soc. 63*, 289–307.

Randel, W. J. 1987a. Global atmospheric circulation statistics. NCAR Tech. Note. NCAR/TN 295 + STR.

Randel, W. J. 1987b. A study of planetary waves in the southern winter troposphere and stratosphere. Part I: wave structure and vertical propagation. *J. Atmos. Sci. 44*, 917–935.

Reed, R. J. 1950. The role of vertical motions in ozone-weather relationships. *J. Meteor. 7*, 263–267.

Schoeberl, M. R. and Krueger, A. J. 1983. Medium scale disturbances in total ozone during Southern Hemisphere summer. *Bullt. Amer. Met. Soc. 64*, 1358–1365.

"U.S. Standard Atmosphere", 1976, U.S. Gov. Print. Off., Washington, D.C. Ziemke, J. R. and Stanford, J. L. 1990. One to two month oscillations in the stratosphere during southern winter. *J. Atmos. Sci. 47*, 1778–1793.